

EXPERIMENTAL AND ANALYTICAL ANALYSIS OF FRICTION STIR PROCESSING PROCESS

WEĞLOWSKI Marek Stanislaw

Institute of Welding, Gliwice, Poland, EU, marek.weglowski@is.gliwice.pl

Abstract

The effects of rotational and travelling speeds and down force on the torque in Friction Stir Processing (FSP) process are presented. The relationship between the rotational speed and torque was modelled by an exponential function. The dependence of the travelling speed and down force affecting the torque was successfully approximated by the linear functions. To find a dependence combining the spindle torque acting on the tool with the rotational speed, travelling speed and the down force, the RSM methods was applied. Studies have shown that the increase of the rotational speed causes decrease of the torque and the increase of the travelling speed causes the increase of the torque at the same time. Tests were conducted on casting aluminum alloy AISi9Mg. The experimental results and calculation were compared.

Keywords: Friction Stir Processing, cast aluminum alloy, response surface methodology.

1. INTRODUCTION

A few modification techniques to refine the microstructure of cast aluminum alloys are available. The first group of methods is based on the modification of the morphology of Si particles. In these technologies, modification of chemical composition and thermal treatment can be adopted to modify the coarse acicular Si particles to fine, globular shapes. The second group of techniques refine the coarse primary aluminum phases. Heat treatment at a high temperature for a short time substantially refines the aluminum dendrites in a semisolid processed Al-Si alloys. These modification and heat-treatment techniques, however, cannot effectively eliminate the porosity in Al - Si, nor redistribute the Si or others particles uniformly into the aluminum matrix [1]. Other processes such as squeeze casting [2] or vibration [3] are also useful in improving the cast aluminum properties. The refinement of the microstructure can also be obtained by electromagnetic stirring [4]. However, a more effective modification technique for microstructural modification of cast aluminum alloy is friction stir processing (FSP), which was developed on the basis of friction stir welding (FSW).

During the FSP process, a rotating tool which consists of a pin and a shoulder is used. Sometimes the tool without pin can be applied. The rotating pin plunged into the modified material, is traversing in the desired direction, while the shoulder is acting on the surface and generating enough heat (remains solid state) to soften the material under the tool. The mechanical stirring caused by the plunged rotating pin forces the softened material to undergo intense plastic deformation yielding a processed zone characterized by dynamically recrystallized fine grain structure [5]. It should be noted that the friction processes can be used to joining the metallic materials as well as thermoplastics composites [6-8].

The research into the FSP of surface layers, so far has been focused mainly on the metallurgical analysis of microstructural changes in modified aluminium alloys [9]. However, from a practical point of view it is important to determine the impact of FSP conditions, i.e. a tool rotational speed, travelling speed, down force as well as the shape and type of tool on the moment acting on the tool, temperature in the stirring area, and the amount of heat generated in the stirring area. The heat generated in the area being processed and the level of plastic strain are factors having a decisive effect on microstructural changes, and, consequently, on the mechanical and functional properties of newly formed areas [9, 10].

Many different methods can be used to analyse the FSP process. Among other experimental techniques [11], analytical modelling [11, 12], finite element analysis [13, 14] and neural network techniques [15] are applied.

One of the most interesting way is to use the response surface methodology [16]. The goal of the presented work is to estimate the relationship between FSP parameters such as rotational and travelling speed, down force, and spindle torque. The experimental results are compared with results obtained from the response surface methodology models.

2. EXPERIMENT

The FSP was conducted on a welding machine built on the base of a conventional vertical milling machine. The machine was equipped with an appropriate device for measuring torque and forces (down force and travelling force). The mean value of the spindle torque was measured by the LOWSTIR head and calculated from 100 points in the area of the fully stabilized FSP process. The cylindrical FSP tools was made of HS6-5-2 high speed steel. The first tool was without a pin and the diameter of a shoulder was 20 mm. The second tool was machined to have a shoulder diameter of 20 mm, pin diameter 8 mm, and pin depth 4.5 mm. In addition, the pin had a spiral groove. The roughness and surface quality of test plates were like after milling. The plates were not cleaned. To control the quality of the modified surface, the direct visual testing was carried out. The workpiece was clamped tightly to an 8 mm thick plate made of plain carbon steel which served as a reinforcement, and then fixed to the machine table. In the present investigation, a cast AlSi9Mg material was processed using 30 different combination of tool rotation (in the range of from 112 to 1800 rpm) and travelling speed (in the range of 112 to 1120 mm·min⁻¹). The maximum travelling speed of the milling machine was 1120 mm·min⁻¹. The minimum speed below 112 mm·min⁻¹ was too low due to the efficiency of FSP process. Each of these processes involved a traverse approximately 180 mm in length. The tool tilt angle was kept constant at 1.5°.

3. RESULTS ANS DISCUSSION

It should be noted that the signals recorded during FSP are depended on tool geometry, parameters of the process, parent material, measurement system as well as cooling and clamping system. The influence of the rotational and travelling speeds on the torque acting on the tool is shown in **Fig. 1** and **Fig. 2**, respectively. The data for rotational speed have been least square fitted with semiempirical relation:

$$M = a \cdot \exp\left(-\frac{\omega}{b}\right) + c \quad (1)$$

Function $M(\omega)$ is presented in **Fig. 1**, the results of calculations with equation (1) are given in **Tables 1** and **2**. The data for travelling speed have been least square fitted with linear empirical relation. The results are presented in **Fig. 2** and calculations in **Tables 3** and **4**. The fitting is rather good.

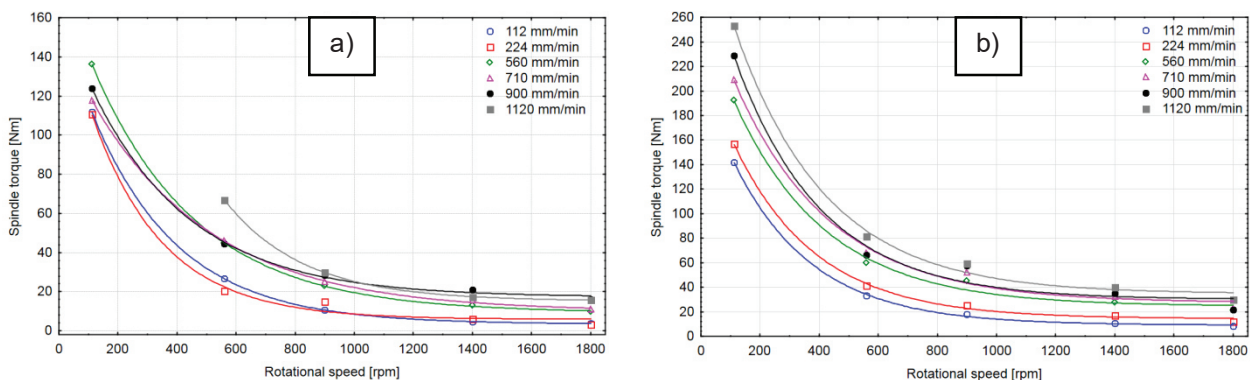


Fig. 1 Influence of rotational speed on the spindle torque acting on the tool, a) without pin, b) with pin

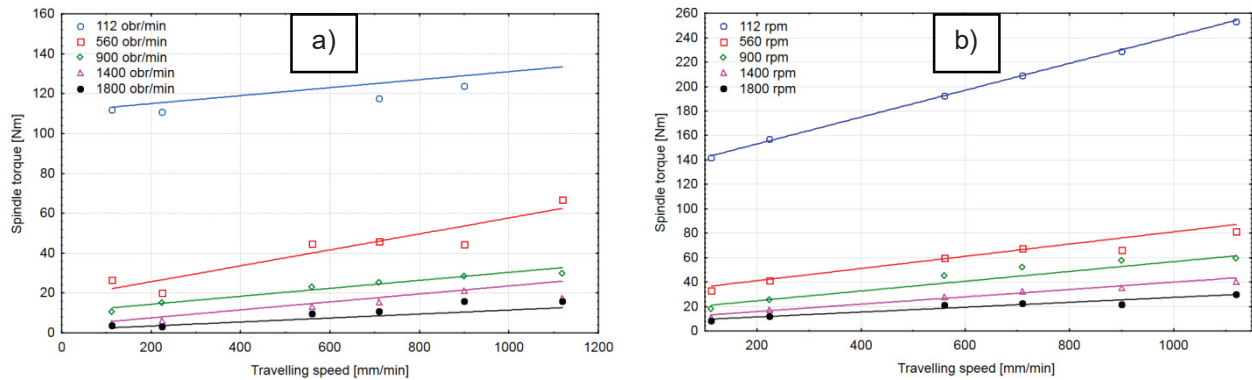


Fig. 2 Influence of travelling speed on the spindle torque acting on the tool, a) without pin, b) with pin

Table 1 Fitted values of the exponential dependence of spindle torque and rotational speed for the selected travelling speed, the function is presented in **Fig. 1a**

Parameter	Travelling speed, mm/min					
	112	224	560	710	900	1120
a, Nm	159.38±0.16	166.02±13.68	174.33±0.99	141.92±1.53	148.69±4.00	417.45±5.03
b, mm·min ⁻¹	290.60±0.67	242.69±42.27	353.71±5.14	408.06±11.80	336.68±22.45	268.23±1.61
c, Nm	3.39±0.05	5.85±3.03	9.16±0.44	9.84±0.83	17.19±1.63	15.20±0.07
R ²	1.00	0.99	0.99	0.99	0.99	0.99

Table 2 Fitted values of the exponential dependence of spindle torque and rotational speed for the selected travelling speed, the function is presented in **Fig. 1b**.

Parameter	Travelling speed, mm/min					
	112	224	560	710	900	1120
a, Nm	186.42±15.11	192.74±23.54	225.97±24.39	241.61±30.16	278.71±19.92	312.58±16.49
b, mm·min ⁻¹	344.19±69.91	416.39±137.85	438.33±131.15	491.98±178.97	342.78±61.28	310.14±39.28
c, Nm	7.20±6.41	9.53±13.27	17.35±14.80	16.57±21.49	27.23±8.39	34.14±39.28
R ²	0.98	0.94	0.95	0.94	0.98	0.99

Table 3 Fitted values of the linear dependence of spindle torque and travelling speed for the selected rotational speed, the function is presented in **Fig. 2a**

Parameter	Rotational speed, rpm				
	112	560	900	1400	1800
a, Nm·mm·min ⁻¹	0.02±0.01	0.04±0.01	0.02±0.002	0.02±0.003	0.01±0.002
b, Nm	111.05±8.79	17.66±5.53	10.36±1.46	3.54±2.13	1.46±1.19
R ²	0.09	0.83	0.94	0.84	0.93

Table 4 Fitted values of the linear dependence of spindle torque and travelling speed for the selected rotational speed, the function is presented in **Fig. 2b**.

Parameter	Rotational speed, rpm				
	112	560	900	1400	1800
a, Nm·mm·min ⁻¹	0.11±0.0	0.05±0.0	0.04±0.0	0.03±0.0	0.02±0.0
b, Nm	131.04±0.83	30.52±2.21	16.75±3.81	9.95±1.76	7.08±1.07
R ²	0.99	0.98	0.92	0.96	0.98

As can be seen the spindle torque acting on the working tool strongly depends on the rotational speed and weakly depends on the travelling speed. This is due to the fact that the rotational speed stimulates the process's temperature [8] as well as volume of modified material [6]. Temperature increases linearly with the increase of the rotational speed, especially for tool with pin [10]. Hence, the friction coefficient can be lower. However, it should be noted that for higher temperature (typical for FSP process) at a higher friction velocity, the friction coefficient can be constant. It would be expected that this decreases the torque. The second issue is that increase of the temperature causes the increase the plasticity of the material. So, higher temperature causes a decrease in the material resistance for the travelling tool. However, the torque is less affected by the change in the travelling speed. Such behavior can be rationalized when assuming that for a constant rotational speed and decreasing travelling speed, the volume of material being processed per each tool revolution decreases, hence the heat is generated in a smaller volume, and this in turn may lead to rise in the temperature and decrease in the flow stress. Modest influence of the travelling speed on the torque is likely caused by a weaker relation between the travelling speed and temperature compared to the influence of the rotational speed on temperature. During the experiments, the penetration depth was kept constant (control by the machine operator). Hence, the value of the down force depends on rotational and travelling speeds and also machine operator.

The value of spindle torque is influenced by rotational speed, travelling speed, down force, type and shape of the tool, and the kind of modified material. The response surface methodology (RSM) has been applied in order to find a dependence combining the torque acting on the tool with the rotational speed in a wider range (112÷1800 rpm), the travelling speed in the range of 112÷1120 mm·min⁻¹ and down force. RSM has been built in Statistica software. Rotational and travelling speeds and down force were introduced as independent variables. A first order response surface models were used during mathematical modeling. The interactions between the independent variables were assumed in the model.

In order to determine the relationship between parameters and torque based on RSM, a linear model was assumed as:

$$M = B_0 + B_1 \cdot \omega + B_2 \cdot v + B_3 \cdot F_d + B_4 \cdot \omega \cdot v + B_5 \cdot \omega \cdot F_d + B_6 \cdot v \cdot F_d \quad (2)$$

The calculation results of the regression coefficients for the linear model are shown in **Table 5**. The calculation results indicate the significance level p where linear main effects are statistically significant (p < 0.05), suggesting that a linear model containing the interaction is sufficient. The comparison between experimental results and calculation are presented in **Fig. 3**.

Table 5 Results of calculation of regression coefficients for linear model (rounding of the number)

The regression coefficients	Results for tool No 1 without pin		Results for tool No 2 with pin	
	Values	Probability - p	Values	Probability - p
B0	34.9501	0.1001	-13.3548	0.0
B1	-0.0191	0.1372	-0.0019	0.0
B2	-0.0153	0.6070	-0.0428	0.0048
B3	4.25299	0.0024	6.6789	0.0001
B4	0.00003	0.1057	0.0000	0.0179
B5	-0.00423	0.0043	-0.0031	0.0017
B6	-0.000002	0.9987	-0.0013	0.0106

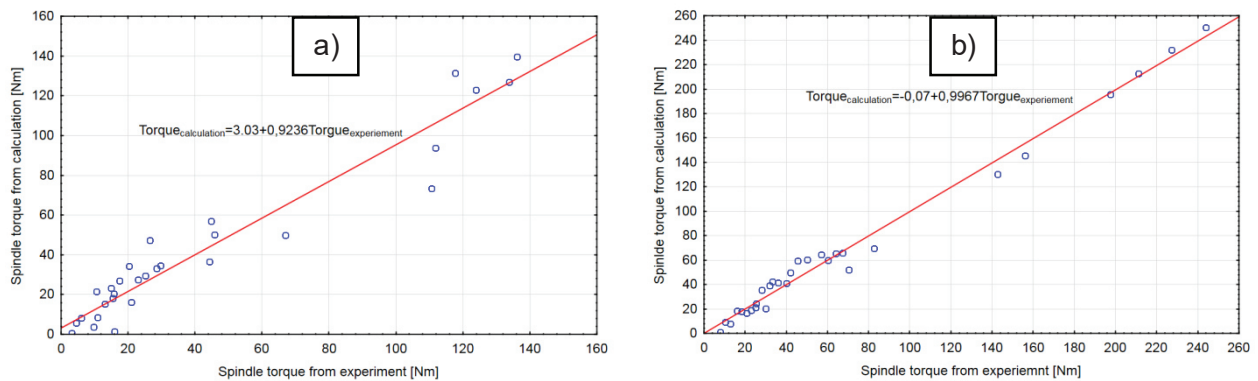


Fig. 3 Comparison between experimental results and calculations, a) tool without pin, b) tool with pin

The typical light microscope microstructure of the processed material is shown in **Fig. 4**. Two well-defined regions could be easily distinguished: the parent material and the FSP area. The parent material was characterized by the coarse grained structure with pores, while the microstructure in the processed zone was modified by the tool action. The result of modification in the processed area was refinement of the microstructure. Further, the porosity in the as cast AISi9Mg sample was nearly eliminated by FSP. The principal microstructural components of this alloys in as-cast state are (Al) dendrites and (Al)+(Si) eutectic. The light microscopy examination revealed characteristic dendrites in the base material (**Fig. 5a**). In the FSP area (**Fig. 5b**), the broken Si particles have a size ranging from submicron to more than ten micrometers.

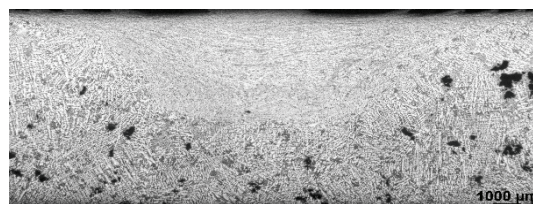


Fig. 4 Typical cross-section of the processed surface area; light microscope, ($\omega=560$ rpm, $v=560$ mm/min)

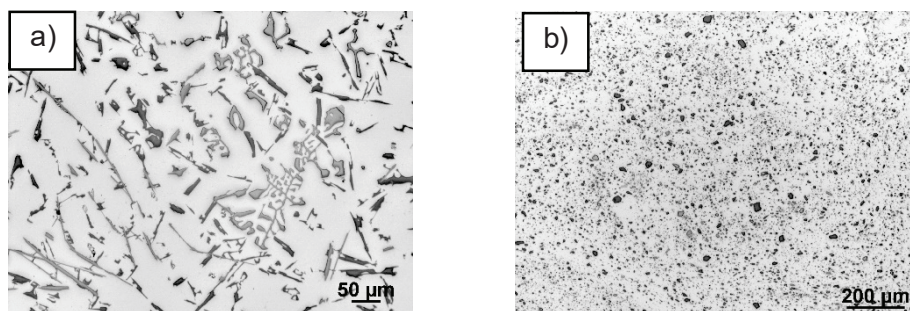


Fig. 5. Micrograph of a) parent material, b) modified material,

4. CONCLUSION

The present study has examined the relationship between parameters of FSP process and spindle torque, and microstructure of a modified AISi9Mg alloy. The conclusions are as follows:

- the increase in the rotational speed decreases the torque acting on the tool,
- the increase in the travelling speed increases the torque acting on the tool,

- the relationship between rotational speed and spindle torque can be fitted by the exponential function, while for travelling speed by the linear one,
- the response surface methodology is a useful technique to determine the impact of the parameters of the process on the spindle torque. In this study, a linear models with interaction were used for fitting,
- friction stir processing of the cast AlSi9Mg aluminum alloy resulted in a significant change in microstructure. Fracturing of coarse acicular Si particles and primary aluminum dendrites and elimination of cast porosity produced a homogeneous microstructure.

REFERENCES

- [1] MA Z.Y., SHARMA S.R., MISHRA R.S. Microstructural Modification of As-Cast Al-Si-Mg Alloy by Friction Stir Processing. *Metallurgical and Materials Transactions A: Physical Metallurgy and Materials Science*, Vol. 37, No 11, 2006, pp. 3323-3336.
- [2] CIUCKA T. Influence of Vibration During Crystallization on Mechanical Properties and Porosity of EN AC -AlSi17 Alloy. *Archives of Foundry Engineering*, Vol. 13, No 1, 2013, pp. 5-18.
- [3] ZYSKA A., KONOPKA Z., LAGIEWKA M., NADOLSKI M. Optimization of Squeeze Parameters and Modification of AlSi7Mg alloy. *Archives of Foundry Engineering*, Vol. 13, No 2, 2013, pp. 113-116.
- [4] WROBEL, T., SZAJNAR, J. Modification of pure Al and AlSi2 alloy primary structure with use of electromagnetic stirring method. *Archives of Metallurgy and Materials*, Vol. 58, No 3, 2013, pp. 941-944.
- [5] DARRAS B.M., KHRAISHEH M.K. Analytical Modeling of Strain Rate Distribution During Friction Stir Processing. *Journal of Materials Engineering and Performance*, Vol. 17, 2008, pp. 168-177.
- [6] WEGLOWSKA A. Effect of vibration welding parameters on the quality of joints made of polyamide 66. *Polimery*, Vol. 59, No 3, 2014, pp. 239-245.
- [7] WELOWSKA A., PIETRAS A. Influence of the welding parameters on the structure and mechanical properties of vibration welded joints of dissimilar grades of nylons. *Archives of Civil and Mechanical Engineering*, Vol. 12, 2012, pp. 198-204.
- [8] WEGLOWSKA A. Research into linear vibration welding of glass fibres reinforced nylon 66. *Welding in the World*, Vol. 59, No 3, 2015, pp. 339-352.
- [9] WEGLOWSKI, M.ST., DYMEK, S., Microstructural modification of cast aluminium alloy AlSi9Mg via Friction Modified Processing. *Archives of Metallurgy and Materials*, Vol. 57, No 1, 2012, pp. 71-78,
- [10] WEGLOWSKI, M.ST., DYMEK, S. Relationship between Friction Stir Processing parameters and torque, temperature and the penetration depth of the tool. *Archives of Civil and Mechanical Engineering*, Vol. 13, No 2, 2013, pp. 186-191.
- [11] WEGLOWSKI, M.ST. An experimental study on the Friction Stir Processing process of aluminium alloy. *Key Engineering Materials*, Vols. 554-557, 2013, pp. 1787-1792.
- [12] WEGLOWSKI M.ST., PIETRAS A. Friction Stir Processing - analysis of the process. *Archives of Metallurgy and Materials*, Vol. 56, No 2, 2011, pp. 779-788.
- [13] WEGLOWSKI, M.ST., DYMEK, S., HAMILTON, C., Experimental investigation and modelling of Friction Stir Processing of cast aluminium alloy AlSi9Mg, *Bulletin of The Polish Academy of Sciences-Technical Sciences*, Vol. 61, No 4, 2013, pp. 893-904.
- [14] HAMILTON C., WĘGLOWSKI M.ST., DYMEK S. Simulation of Friction-Stir Processing for Temperature and Material Flow. *Metallurgical And Materials Transactions B*, 2015, DOI: 10.1007/s11663-015-0340-z
- [15] PARADISO V., ASTARITA A., CARRINO L. et al. Numerical optimization of selective superplastic forming of friction stir processed AZ31 Mg alloy. *Key Engineering Materials*, Vols. 554-557, 2013, pp. 2212-2220.
- [16] LAKSHMINARAYANAN A. K., BALASUBRAMANIAN V. Comparison of RSM with ANN in predicting tensile strength of friction stir welded AA7039 aluminium alloy joints. *Trans. Nonferrous Met. Soc. China*, Vol. 19, 2009, pp. 9-18.